EXPERIMENTAL FLOW INVESTIGATION INSIDE AN AXIAL COMPRESSOR WITH ACTIVE FLOW CONTROL

Joseph Moubogha Moubogha **Pierric Joseph** **Olivier Roussette** **Antoine Dazin**

Univ. Lille, CNRS, ONERA, Arts et Métiers Institute of Technology, Centrale Lille, UMR 9014 - LMFL - Laboratoire de Mécanique des Fluides de Lille - Kampé de Fériet, F-59000 Lille, France

ABSTRACT

This paper describes the experimental study of the flow behavior in a rotor blade channel of an axial compressor equipped with an Active Flow Control (AFC) system using Particle Image Velocimetry. The AFC system consists of 40 actuators connected to an auxiliary supply pressure system. It is used to extend the stable operating range and to improve the performance of the compressor. The system is able to generate high speed jets blowing just at the tip of the rotor blades. PIV data are obtained at three radial positions (at 18%, 51% and 79% of the blade height) in the inter-blade channel region. The PIV results are discussed to analyze the effect of the control system on the compressor internal flows.

Keywords: Axial Compressor; Active Flow Control; PIV

NOMENCLATURE

B	Base configuration
C	Controlled configuration
C_x	Axial chord length
X	Axial direction
Y	Tangential direction
PIV	Particle Image Velocimetry
V_x	Axial velocity
V_y	Tangential velocity
ω	Rotor rotational speed (rpm)
r	Radial position of PIV plane
W_{mag}	Magnitude of relative velocity
β	Angle of relative velocity

1. INTRODUCTION

The aerodynamic stall and surge instabilities that develop in axial compressors operating at low flow rates and high pressure ratios represent major flight safety risks as their occurrence can lead to dramatic accidents. Therefore, to the detriment of efficiency, engine manufacturers introduce operational safety margins to prevent the occurrence of these phenomena. This deprives the machines from their higher pressure ratios and higher efficiencies operating points. However, solutions have been developed by researchers to avoid these aerodynamic instabilities and to improve the stall margin (SMI) through flow control. Passive flow control techniques, such as casing treatment [1] can be cited. They involve permanent modification of the casing and sometimes result in efficiency losses even far from the stability limit. Active flow control is another very interesting alternative technique, which can easily be switched on and off, and many research works have been carried out in this area, summarized recently by Li et al [2]. The most common onset of stall in modern engines is the spike type, which is caused by phenomena occurring at the blade tip [3-5]. The most effective way to control these phenomena is therefore to blow a high momentum jet at the tip of the blade, as demonstrated by several authors [6-8], in order to decrease the load and/or to act on the dynamics of the tip vortex. In the extensive literature on this subject, there are however few studies that investigate the effect of active control (most commonly blowing) on the internal flows. One can however mention the study by Margalida et al [9] where the effect of an active flow control system on the mechanisms of occurrence of rotating stall is discussed with a focus on the flow patterns present in the tip region just before stall and how they evolve when active flow control is applied. These analyses were relying on instantaneous pressure measurements at the casing. It should also be said that Particle Image Velocimetry has been remarkably applied to the study of the interaction between the rotor blade tip and the casing treatment in a transonic compressor stage [10]. However, the latter study deals with passive rather than active flow control.

The present paper aims precisely at examining the effect of active flow control on the internal flow of a compressor through an experimental investigation of the flow using Particle Image Velocimetry. The support of this study is a single-stage axial compressor test rig equipped with an active flow control system [9] and a PIV measurement system. After a description of the experimental set-up and instrumentation, the paper will focus on the presentation of the internal flow of the compressor without and with the use of the active flow control system at different operating points of the machine; whether it is the nominal operating point or the last stable operating point without and with control. This work is involved in the *European* Union's Horizon 2020 research project ACONIT [11] that aims at designing, manufacturing and testing actuators for flow control for an implantation in an aircraft engine.

2. EXPERIMENTAL SET-UP

The support of the experiments performed in the present study is the low speed single stage axial compressor CME2 located at Arts et Métiers Institute of Technology in Lille. The compressor is represented in Figure 1 and its main characteristics are given in Table 1.

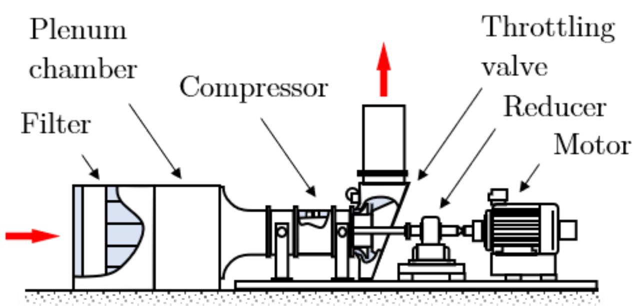

FIGURE 1: TEST BENCH WITH CME2 COMPRESSOR ADAPTED FROM [15]

The compressor has been equipped with an Active Flow Control (AFC) system consisting of 40 actuators connected to an auxiliary supply pressure system. The system aims at extending the stable operating range and performance of the compressor (see [9, 14] for more details).

TABLE 1: COMPRESSOR PARAMETERS

Rotational speed	3200	rpm
Design mass flow rate at 3200rpm	5.3	kg/s
Design axial velocity at leading edge	43	m/s
Rotor blade number	30	
Stator blade number	40	
Casing diameter	550	mm
Hub-tip ratio at leading edge	0.75	
Rotor tip chord	84	mm
Rotor tip stagger angle	54	°
Rotor tip gap	0.5	mm

They are able to generate high speed jet blowing just at the tip of the rotor blades (see Figure 2 adapted from [15]). The opening of each actuator is controlled by an electromagnetic valve. This allows to generate continuous or pulsed jet with frequency up to 200 Hz. With a supply pressure up to 8 bar, each injector pairs can then operate independently and produce jet speed up to 200 m.s^{-1} through a 10 × 0.5 mm² slot. Accordingly, injected mass flow can be adjusted from 0 to about 2.5 % of the main flow rate, either by changing the supply pressure or the duty cycle of the solenoid valves when pulsed injection is used. As stated in literature, blowing is most effective in front of the rotor leading edge [2], and the critical area is located at the tip, close to the casing [3]. Consequently, actuators are located 10 mm upstream of the rotor ($x = -20$ %.Cx where Cx is the axial chord), and injectors are shaped to benefit from the Coandă effect to blow along the casing right in the tip gap [4]. Injectors can also be rotated along their axis to vary the yaw angle of injection and an absolute injection angle of -30° was chosen as it corresponds to the best performance of the compressor in terms of stall margin improvement [5]. The absolute blowing angle is considered negative when the direction of blowing is opposite to the direction of rotation of the rotor. The control strategy chosen and presented in this study corresponds to a continuous blowing with 40 injectors and an injected mass flow rate of 2.5% of the main flow rate. The blowing angle is -30°.

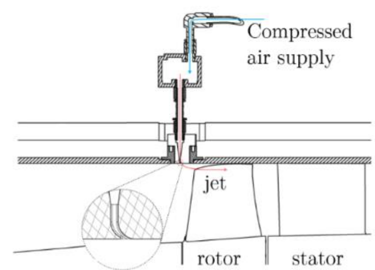

FIGURE 2: ACTIVE FLOW CONTROL SYSTEM ADAPTED FROM [15]

Velocity fields have been measured in a blade channel via an endoscopic 2D – 2C Particles Image Velocimetry (PIV). The PIV system is composed by a multi-pulse Innolas Spitlight Compact 400 PIV (532 nm) laser associated to an articulated mirror arm to guide the laser beam from the source to the endoscope. A cylindrical lens is mounted at the end of the endoscope to generate a laser sheet. The seeding tracer particles of the flow were generated by means of a smoke generator fed with fog fluid. In order to achieve a homogeneous particle distribution, the smoke generator was placed upstream of the compressor inlet section, which resulted in a very good and stable seeding. A Lavision Imager sCMOS camera with a spatial resolution of 2560 × 2160 pixels at an acquisition frame rate of 5 Hz synchronized with the wheel was used. The focal length of the camera lens was f = 60 mm. A calibration target with a 5 x 5 mm² dot grid was used to align the camera object plane with the light sheet plane. To compute the velocity field, an in-house multi-pass algorithm is used on 100 pairs of PIV snapshots recorded during every acquisition (with final interrogation of 32 × 32 pxl^2 with 50% overlap).

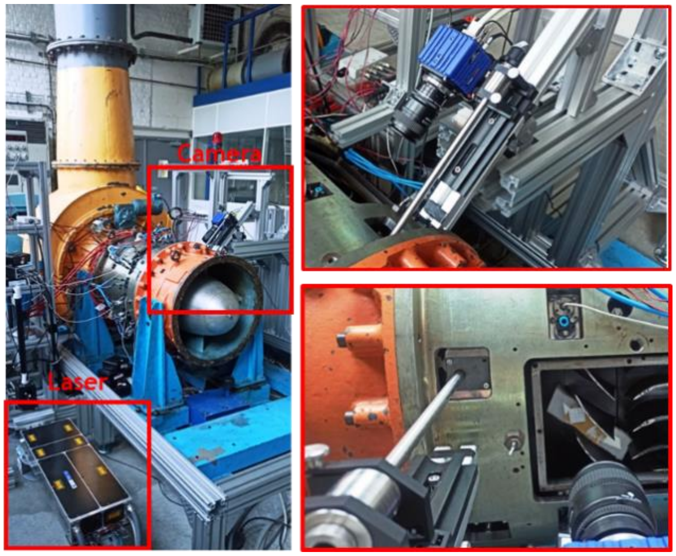

FIGURE 3: DETAILS OF THE PIV SYSTEM

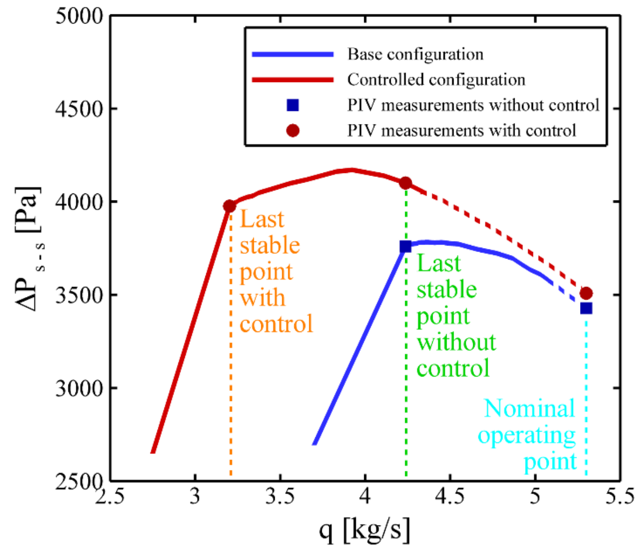

FIGURE 4: PERFORMANCE CURVES OF THE COMPRESSOR WITH PIV MEASUREMENTS IN BASE AND CONTROLLED CONFIGURATIONS

Two transparent visualization windows were installed, one after the other, on the carter of the compressor, above the stage, to have an optical access to the flow, first in the base configuration, then in the controlled configuration. Due to the location of the injectors on the control visualization window, a part of the field of view is lost in the inlet region of the inter-blade rotor channel, as it will be seen in Figures 5 and 6. The PIV measurements were performed on three radial planes at 79%, 51% and 18% of the blade height in base and controlled configurations at different operating points. The mass flow is varied using a throttling valve located downstream to the compressor stage. The performance of the compressor is evaluated thanks to two differential pressure sensors located on the test rig. The first sensor measures the difference between the total pressure recorded in the plenum chamber and a mean static pressure measured at the end of the converging pipe located just downstream to the plenum chamber. The dynamic pressure at compressor inlet is this measured, which allows to evaluate the flow rate. The second one is used to evaluate the stage performance by measuring static pressure in upstream of the rotor and downstream of the stator. The precision of these measurements has been evaluated to ± 0.012 kg.s^{-1} and ± 1.3 Pa for the flow rate and the static-to-static pressure rise, respectively [15]. Figure 4 shows the performance curves of the compressor without and with control, in terms of static to static pressure rise as a function of mass flow. The points for which PIV measurements were performed are highlighted on the same figure. These experiments were conducted for three flow rates :

- The nominal operating point (q = 5.3 kg/s)
- The flow rate corresponding to the last stable point without control (q = 4.3 kg/s).
- The flow rate corresponding the last stable point with control (q = 3.2 kg/s)

3. RESULTS AND DISCUSSION

In the following, the V_x PIV component corresponds to the axial velocity component. The V_y velocity component is the projection of the tangential velocity component in the laser plane. As the maximum angular extension of the laser sheet is small (less than 6°) the projection error is of the order of 1% and the V_y component will thus be considered to be the tangential velocity component in the rest of the paper. The magnitude of the relative velocity is evaluated using the relationship

$$W_{mag} = \sqrt{V_x^2 + (V_y - \omega r)^2} \tag{1}$$

where ω is the rotational speed of the compressor and r the radial position of the laser plane.

3.1 Nominal operating point

The mean relative velocity fields obtained at the nominal operating point on the PIV planes at 79% and 18% of blade height are shown in Figures 5 and 6, in the base and controlled configurations respectively. As expected, in the relative reference frame, the flow entering the inter-blade channel is guided by the rotor blades from the inlet to the outlet with a decrease of the relative flow velocity.

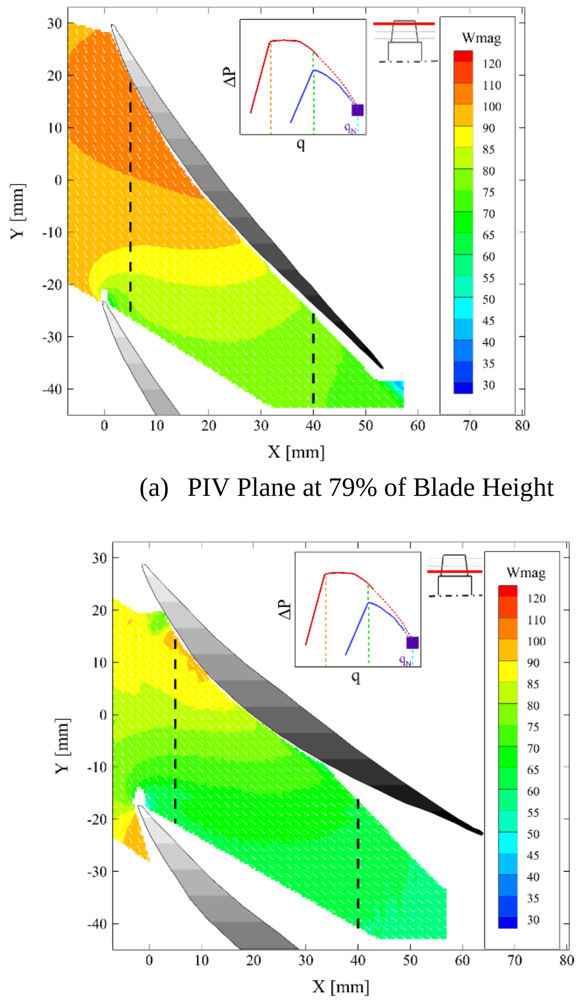

(a) PIV Plane at 79% of Blade Height

(b) PIV Plane at 18% of Blade Height

FIGURE 5: MEAN RELATIVE VELOCITY THE IN BASE CONFIGURATION AT NOMINAL OPERATING POINT ON PIV PLANES AT (a) 79% AND (b) 18% OF BLADE HEIGHT

Comparing the velocity fields of the controlled case with those of the base case, there is clearly an over speed at the blade tip which seems to disappear near the hub. In order to clearly see this, the mean profiles are extracted near the inlet (at x = 5mm that is $x/C_x = 0.09$ with x the distance from the leading edge and c_x, the axial chord at tip) in Figure 7 and close to the rotor outlet (at x = 40 mm that is $x/C_x = 0.73$) in Figure 8. The line on which the profiles are extracted are marked in dashed on the velocity maps Figure 5 and 6. In the legends, B and C refer to the base and controlled cases respectively. The over velocity due to the control can be seen on the inlet and outlet profiles of axial velocity at the blade tip (79%) and at mid-height (51%). Near the hub (18%), the excess velocity is not observed. In fact, as the blowing is concentrated at the casing, the main flow upstream of the injectors is deflected towards the hub in the presence of the injected jets (see Figure 9a), thus reducing the cross sectional area of the main flow and causing the velocity increase. As this takes place at the blade tip, the effect fades close to the hub.

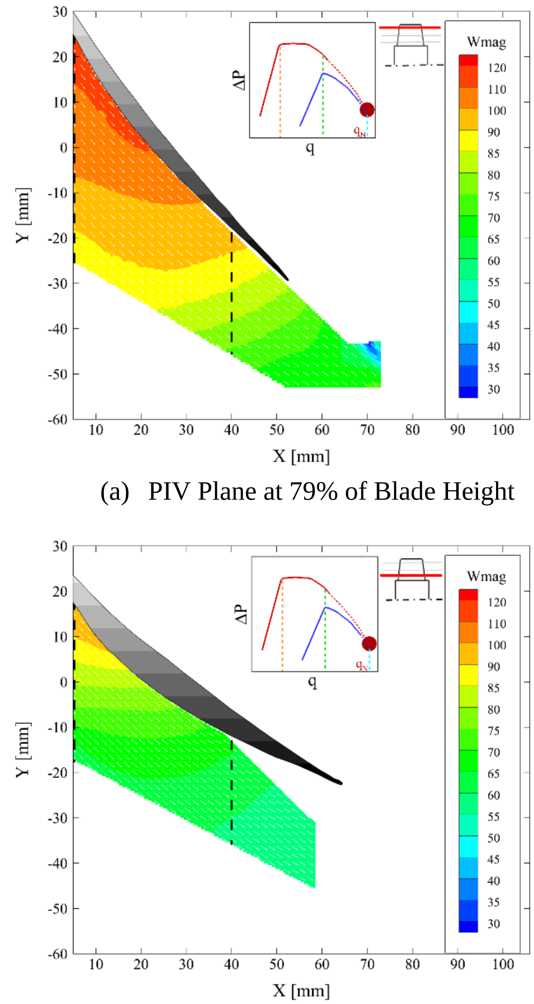

(a) PIV Plane at 79% of Blade Height

(b) PIV Plane at 18% of Blade Height

FIGURE 6: MEAN RELATIVE VELOCITY IN CONTROLLED CONFIGURATION AT NOMINAL POINT ON PIV PLANES AT (a) 79% AND (b) 18% OF BLADE HEIGHT

Concerning the tangential velocity components in Figure 7 and 8, the increase of the tangential velocity with decreasing radial position of the PIV laser plane on the blade height is due to the rotor blades design, which aims at giving the same work over the blade height.

On the controlled case, and compared with the base case, over values of tangential velocities can clearly been observed in Figures 7 and 8 at 51% and 79%. This is more pronounced at mid-height (51%) where this velocity over-value can exceed of more than 25% the base case value. This over value of the tangential velocity disappears near the hub (18%). This phenomenon has a direct impact on the relative flow angle that deviates what can be observed without control (see Figures 7 and 8).

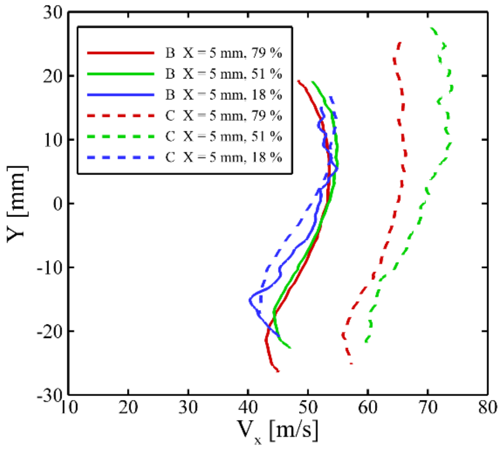

(a) Inlet Axial Velocity

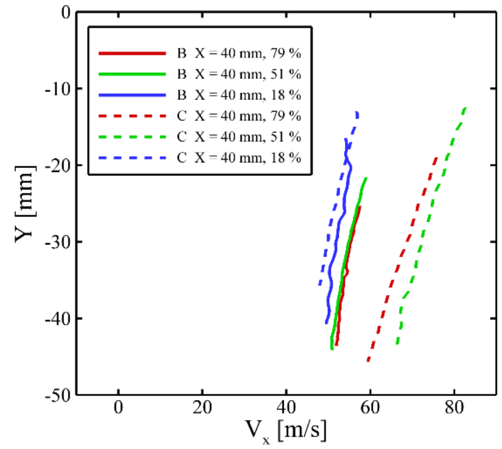

(a) Outlet Axial Velocity

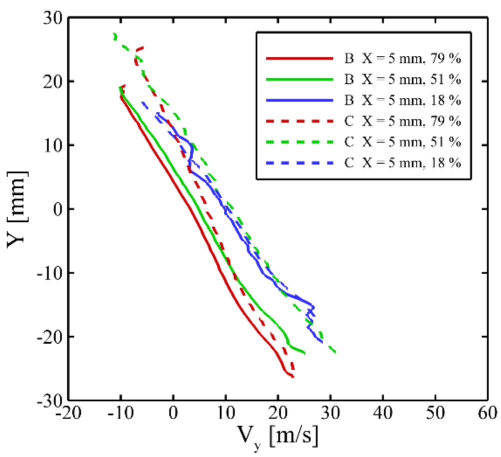

(b) Inlet Tangential Velocity

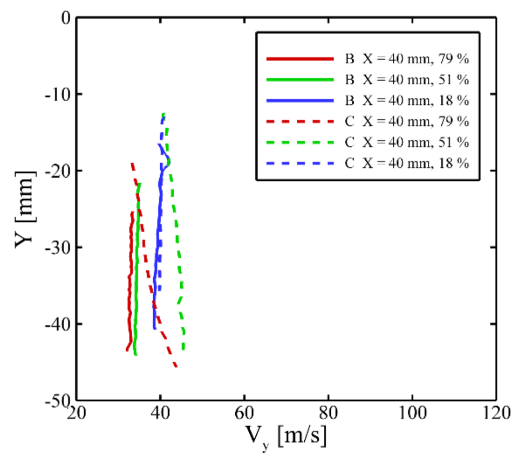

(b) Outlet Tangential Velocity

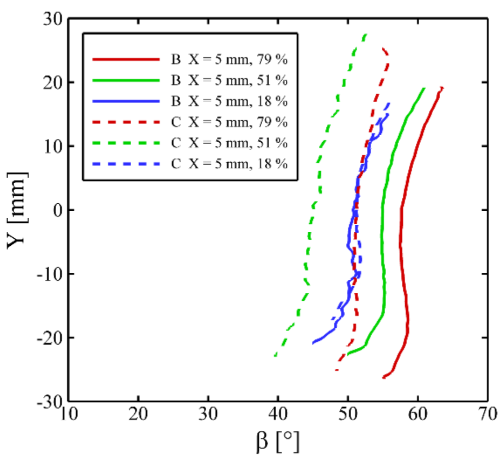

(c) Inlet Relative Angle

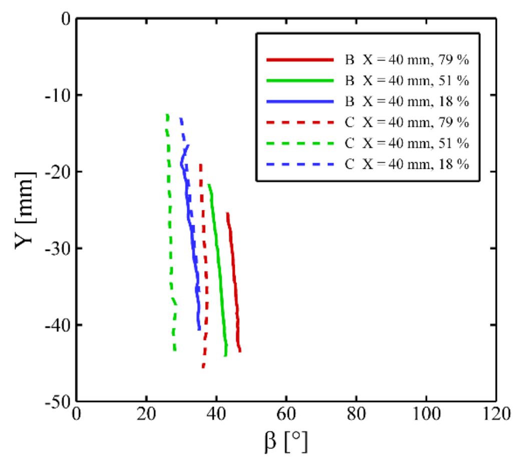

(c) Outlet Relative Angle

FIGURE 7: MEAN PROFILES AT NOMINAL OPERATING POINT IN BASE (B) AND CONTROLLED (C) CONFIGURATIONS AT $X/C_X = 0.09$

FIGURE 8: OUTLET AT NOMINAL OPERATING POINT IN BASE (B) AND CONTROLLED CONFIGURATIONS (C) $X/C_X = 0.73$

It is reminded that the jet is blowing at high velocity in a direction opposite to the rotating direction at casing. Associated to the over tangential velocity component observed, especially at mid blade height, we can infer that an axial swirling flow is created in the blade channel, as illustrated in Figure 9b. This swirling region is occupying a large zone of the channel from the casing to, at least, channel mid-height but is not affecting the region close to the hub.

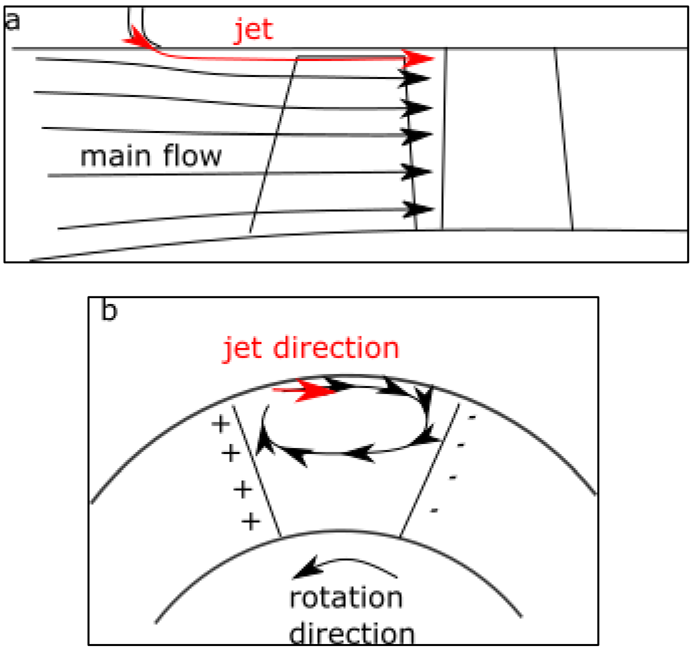

FIGURE 9: BLOWING EFFECT ON THE FLOW IN THE ROTOR BLADE CHANNEL, IN THE MERIDIONAL PLANE (a) AND IN THE PLANE NORMAL TO THE ROTATION AXIS(b)

3.2 Last stable operating point without control

The mean relative velocity fields at a flow rate corresponding to the last stable operating point without control (q=4.3 kg/s), at 79% and 18% of the blade height are presented in Figures 10 and 11, in the base and controlled configurations respectively. The main difference between these velocity fields and those obtained at the nominal operating point (shown in Figures 5 and 6) is the appearance of a region of low relative velocity developing from mid-chord, on the blade suction side where the flow seems detached. Comparing the flow fields in the base case to those in the controlled case, the detached flow region appears wider and more extensive at the exit of the inter-blade channel in the latter.
In Figure 12, the profile of axial velocity, tangential velocity and relative angle are compared, close to the outlet, in the base and controlled cases. The inlet profiles are no longer presented here and in the following since their evolution corresponds quite typically to the one described from the inlet profiles obtained at the nominal operating point in Figure 7. Considering the outlet axial velocity achieved at the last stable operating point without blowing (see Figure 12 a) and comparing it to the one achieved at the nominal operating point (see Figure 8 a), a global decrease of the velocity is observed as expected. The over speed effect due to control already highlighted at the nominal operating point is also visible at the last stable operating point without blowing. And the signature of the detached flow region is evidenced on the axial velocity profiles by the change in slope of the profiles and the abrupt drop in velocity.
Regarding the tangential velocity profiles, comparing Figures 8 b and 12 b, an increase in tangential velocity from the nominal operating point to the last stable operating point without blowing is observed, as expected, leading to an increase of the work done by the blade, as usually observed, at partial flow rates.
Similarly to what was observed at the nominal point, and according to the flow mechanism describe in Figure 9b, the blowing leads to an over-value of the tangential velocity component (Figure 12b). The detached flow region is characterized here by the beginning of the change in slope of the profiles and by a very clear increase in tangential velocity that is approaching the rotational speed of the blades at the different radial positions, respectively 87 m/s, 81 m/s and 73 m/s for 79%, 51% and 18% of the blade height. On this plot, the detached region appears also to be larger in the controlled case. This can be linked to the over value of the work done by the blade, which leads to an additional adverse pressure gradient which promotes the detachment on the blade suction surface.

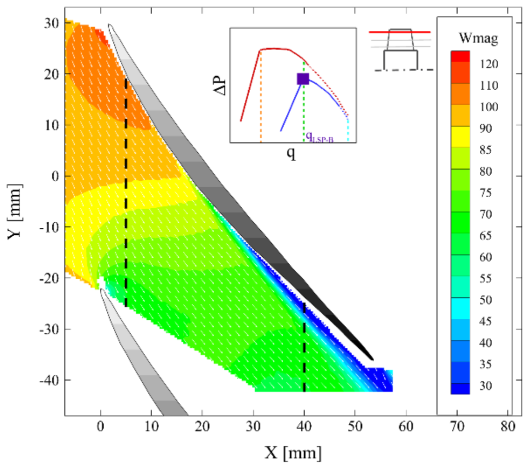

(a) PIV Plane at 79% of Blade Height

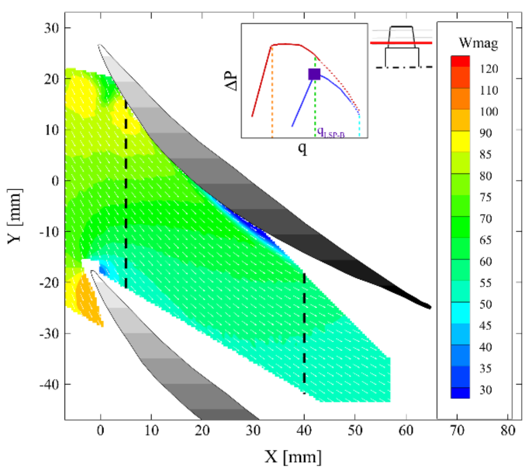

(b) PIV Plane at 18% of Blade Height

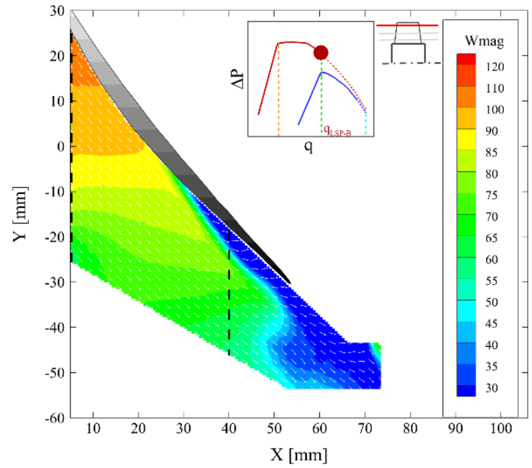

(a) PIV Plane at 79% of Blade Height

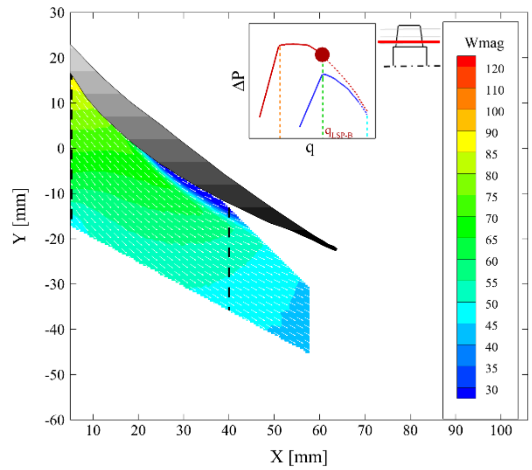

(b) PIV Plane at 18% of Blade Height

FIGURE 10: MEAN RELATIVE VELOCITY IN BASE CONFIGURATION AT LAST STABLE OPERATING POINT WITHOUT CONTROL ON PIV PLANES AT (a) 79% AND (b) 18% OF BLADE HEIGHT

FIGURE 11: MEAN RELATIVE VELOCITY IN CONTROLLED CONFIGURATION AT LAST STABLE OPERATING POINT WITHOUT CONTROL ON PIV PLANES AT (a) 79% AND (b) 18% OF BLADE HEIGHT

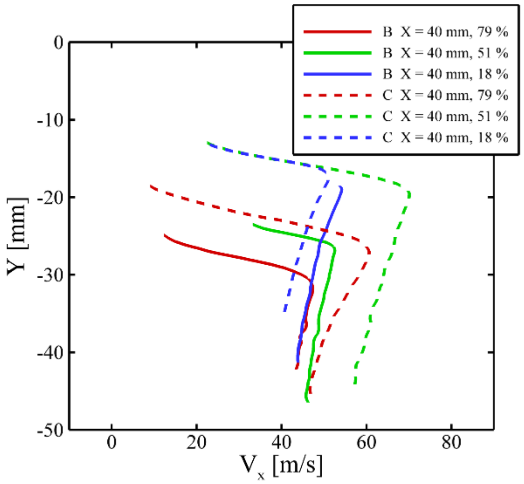

(a) Outlet Axial Velocity

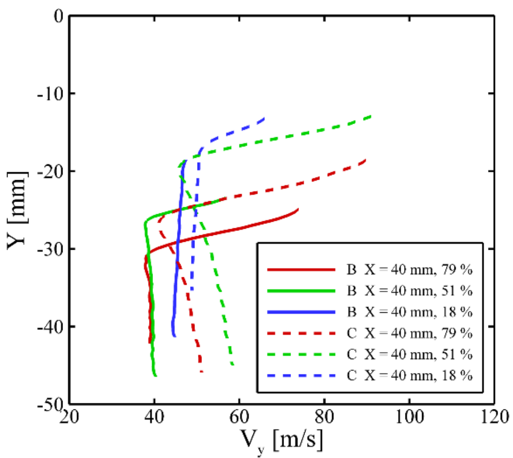

(b) Outlet Tangential velocity

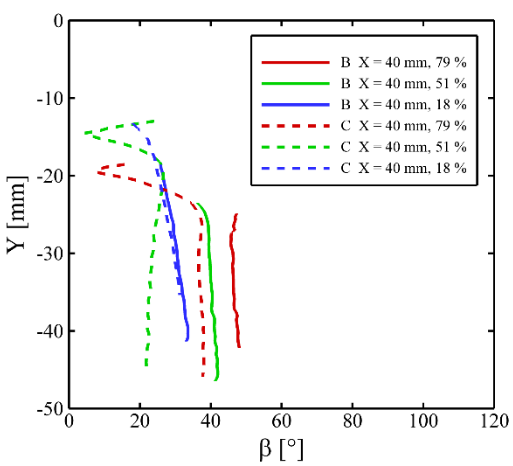

(c) Outlet Relative Angle

FIGURE 12: OUTLET MEAN PROFILES AT LAST STABLE OPERATING POINT WITHOUT CONTROL (q=4.3 kg/s) IN BASE AND (B) CONTROLLED (C) CONFIGURATIONS

3.3 Last stable point with control

Finally, the average of the relative velocity fields and velocity vectors obtained at the last stable operating point with control on the PIV planes at 79%, 51% and 18% of the blade height are shown in Figure 13. A very large detached flow region extends, from tip to hub. The channel near the blade tip is completely blocked at 79% of the blade height, whereas it has as a smaller extent in the blade to blade direction when going closer to the hub. What is remarkable, compared to the last stable point without control (figure 10), and in spite of the large detached region describe above, is that the compressor is not stalled.
In Figure 14, the velocity profiles of the axial and tangential velocity and the angle of the relative velocity with respect to the axial direction are plotted for this operating point. They are compared to the ones obtained at the last stable operating point without control to evaluate the differences we have on the flow just before rotating stall arising in both cases. From the velocity profiles (see figure 14 a and b) we can confirm that in the controlled case the inter-blade channel is blocked at 79% of the blade height as there is no outflow since the axial velocity is nearly null. The corresponding tangential velocity is tending to the value of the blade velocity. The flow is therefore deviated and accelerated at the lowest blade heights where the inter-blade channel is not completely blocked, as can be seen at 51% and 18% of the blade height. At these two heights, and especially at 18%, there are still regions close to the pressure side of clearly positive axial velocities associated with high value of the tangential velocity component. These are thus regions where the compressor is able to produce a good amount of work.
What has been shown in [9] is that the compressor under study is tip critical and that the tip blowing is completely preventing the phenomena at the origin of the rotating stall and occurring at tip to develop. Therefore, the blowing allows the compressor to operate at lower flow coefficient, with higher incidence at rotor inlet (at least on a large part of the blade height), and with a strong adverse pressure gradient. This leads to large detachments in the blade channel as illustrated in Figures 13 and 14 and to completely different transition to rotating stall.

4. CONCLUSION

The present study reports the results of a Particle Image Velocimetry technique application for examining the effect of active flow control on the internal flow of a compressor. The experimental investigation was conducted on a single stage axial compressor test-bench. The machine is equipped with fluidic actuators installed on the casing upstream of the rotor. PIV measurements were performed on the three radial planes at 79%, 51% and 18% of the blade height and at the nominal and very near stall operating points in the base and controlled configurations.

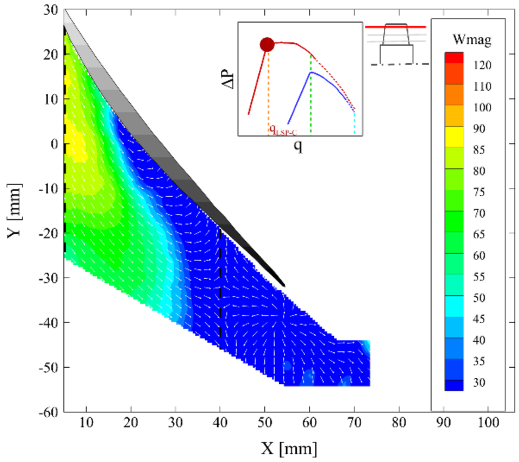

(a) PIV Plane at 79% of Blade Height

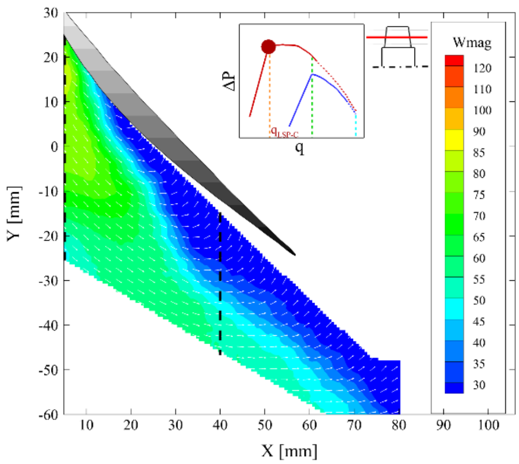

(b) PIV Plane at 51% of Blade Height

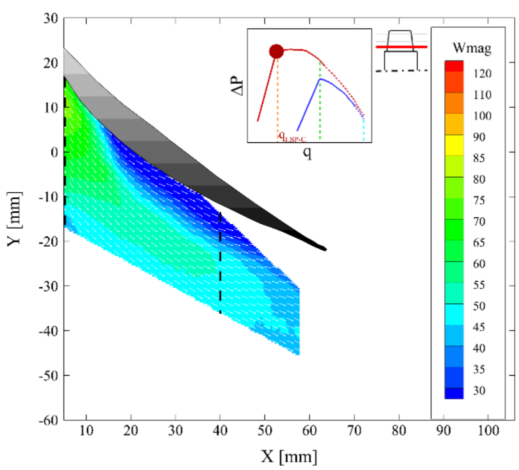

(c) PIV Plane at 18% of Blade Height

FIGURE 13: MEAN RELATIVE VELOCITY IN CONTROLLED CONFIGURATION AT LAST STABLE OPERATING POINT WITH CONTROL

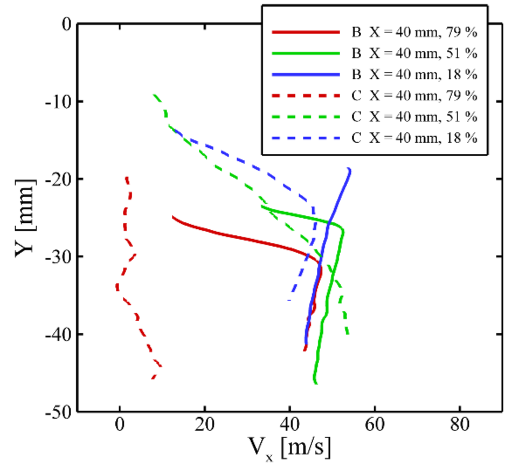

(a) Outlet Axial Velocity

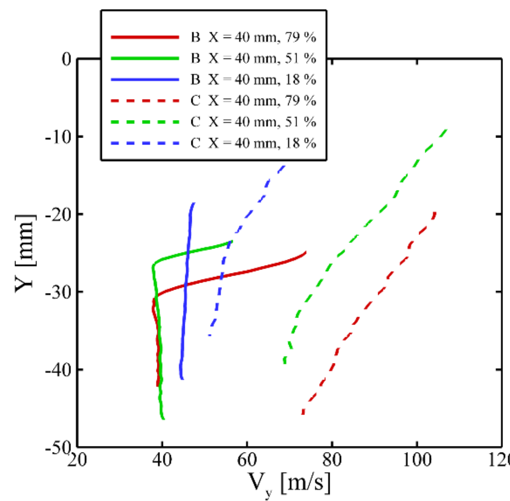

(b) Outlet Tangential Velocity

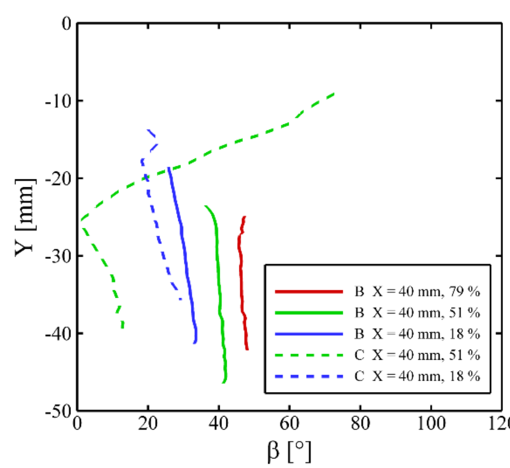

(c) Outlet Relative Angle

FIGURE 14: OUTLET MEAN PROFILES AT LAST STABLE OPERATING POINT IN BASE (B – q=4.3 kg/s) AND CONTROLLED (C – q=3.2 kg/s) CONFIGURATIONS

It appears that the effect of the control system is to accelerate the internal flow with the appearance of a significant over speed at the blade tip, which gradually fades as it approaches the blade root. This is associated to a swirling flow in the plane normal to the axial direction that creates tangential over-velocities on a part of the blade height. This produce additional work, and adverse pressure gradient, which promotes a detachment on the blade suction side. The blowing is also preventing the phenomenon, occurring normally at tip, and leading to rotating stall to develop. This allows the compressor to operate at high incidence, and with a large detachment, which extends over the entire blade height and which is obstructing the inter-blade channel close to tip.

ACKNOWLEDGEMENTS

This paper is supported by European Union's Horizon 2020 research and innovation program under grant agreement No 886352, project ACONIT.

The authors would like to thank the technical staff at Arts et Métiers Institute of Technology in Lille and colleagues at Laboratoire de Mécanique des Fluides in Lille (C. Cuvier from Ecole Centrale and JC Monnier from ONERA) for the technical support and expertise provided during the PIV test campaign. The authors would like also to thank Pr. Gerard Bois for the useful discussions on these results.

REFERENCES

[1] Hathaway, Michael D. Passive Endwall Treatments for Enhancing Stability. *NASA Report No. TM-2007-214409* (July 2007).

[2] Li Jichao, Juan Du, Chaoqun Nie, and Hongwu Zhang. Review of Tip Air Injection to Improve Stall Margin in Axial Compressors. *Progress in Aerospace Sciences* 2019, 106, 15–31.

[3] Hewkin-Smith M., Pullan G., Grimshaw S. D., Greitzer E. M., and Spakovszky Z. S. The Role of Tip Leakage Flow in Spike-Type Rotating Stall Inception. *Journal of Turbomachinery* 2019**,** 141(6).

[4] Pullan G., Young A. M., Day I. J., Greitzer E. M., and Spakovszky Z. S. Origins and Structure of Spike-Type Rotating Stall. *Journal of Turbomachinery* 2015, 137(5)

[5] Day I. J. Stall, surge, and 75 years of research. *Journal of Turbomachinery* 2016, 138(1), 011001.

[6] Kefalakis M, and K D Papailiou. Active Flow Control for Increasing the Surge Margin of an Axial Flow Compressor. *Turbo Expo: Power for Land, Sea, and Air* 2006**,** Vol. 424,101-111.

[7] Stößel, Marcel, Stefan Bindl, and Reinhard Niehuis. Ejector Tip Injection for Active Compressor Stabilization. *Turbo Expo: Power for Land, Sea, and Air, American Society of Mechanical Engineers* 2014**,** Vol. 45608, V02AT37A004.

[8] Suder K. L., Hathaway M. D., Thorp S. A., Strazisar A. J., and Bright M. B. Compressor Stability Enhancement Using Discrete Tip Injection. *Journal of Turbomachinery* 2001, 123(1), 14–23.

[9] Margalida Gabriel, Pierric Joseph, Olivier Roussette, and Antoine Dazin. Active Flow Control in an Axial Compressor for Stability Improvement: On the Effect of Flow Control on Stall Inception. *Experiments in Fluids* 2021**,** 62(1), 1-13.

[10] Voges M., Willert C., Schnell R., Müller M. W.,and Zscherp, C. PIV application for investigation of the rotor blade tip interaction witha casing treatment in a transonic compressor stage. *14th Int Symp on Applications of Laser Techniques to Fluid Mechanics*, July 07-10, 2008, Lisbon, Portugal.

[11] Dazin A., Joseph P., Romano F., Gallas Q., Marty J., Aigouy G., Stößel M., and Niehuis R. The ACONIT Project: An Innovative Design Approach of Active Flow Control for Surge Prevention in Gas Turbines. In *IOP Conference Series: Materials Science and Engineering* 2021**,** 1024(1), 012068.

[12] Nie Chaoqun, Gang Xu, Xiaobin Cheng, and Jingyi Chen. 2002. Micro Air Injection and Its Unsteady Response in a Low-Speed Axial Compressor. *J. Turbomach.* 2002, 124(4), 572-579.

[13] Strazisar A. J., Bright M. M., Thorp S., Culley D. E., and Suder K. L. Compressor Stall Control Through Endwall Recirculation. *Turbo Expo: Power for Land, Sea, and Air* 2004**,** Vol. 41707, 655-667.

[14] Joseph Moubogha Moubogha, Gabriel Margalida, Pierric Joseph, Olivier Roussette, Antoine Dazin. Surge Margin Improvement by Continuous and Pulsed Tip injection. *Proceedings of 14th European Conference onTurbomachinery Fluid dynamics and Thermodynamics ETC14*, April 12-16 2021; Gdansk, Poland.

[15] Margalida Gabriel. Analyse Expérimentale et Contrôle Actif de l'écoulement Dans Un Compresseur Axial Mono-Étagé Durant La Transition Vers Le Décrochage Tournant, *Phd thesis, Ecole Nationale Supérieure d'Arts et Métiers*, 2019.